Two-way shape memory effect of a Ti rich NiTi alloy: experimental measurements and numerical simulations

2007 Smart Mater. Struct. 16 771

(http://iopscience.iop.org/0964-1726/16/3/026)

IOP Publishing Smart Materials and Structures
Smart Mater. Struct. **16** (2007) 771–778 doi:10.1088/0964-1726/16/3/026

Two-way shape memory effect of a Ti rich NiTi alloy: experimental measurements and numerical simulations

A Falvo, F Furgiuele and C Maletta

Department of Mechanical Engineering, University of Calabria, Arcavacata di Rende (CS), Italy

E-mail: carmine.maletta@unical.it

Received 8 November 2006, in final form 7 March 2007
Published 27 April 2007
Online at stacks.iop.org/SMS/16/771

Abstract
In this paper the two-way shape memory effect (TWSME) of a Ni–51 at.% Ti alloy is investigated and a numerical model is developed, which allows real time simulations of its hysteretic behaviour strain versus temperature. The two-way shape memory effect (TWSME) was induced through a proper thermo-mechanical training, carried out at an increasing number of training cycles and for two values of training deformation. The TWSME was measured under different applied stresses and the hysteretic behaviour in the strain–temperature response was recorded. In order to evaluate the thermal stability of the hysteresis loops the material was subjected to many cycles, by repeated heating and cooling, between A_f (austenite finish temperature) and M_f (martensite finish temperature). The numerical method is based on a phenomenological approach and was developed in a Matlab® function, which calculates the model parameters from a set of experimental data, and a Simulink® model, which is efficient enough for use in real time applications. The accuracy of the proposed model was analysed through systematic comparisons between experimental measurements and numerical predictions.

1. Introduction

NiTi shape memory alloys (SMAs) have seen growing use in recent years in mechanical, medical and aerospace industries, due to their special functional properties, namely the shape memory effect (SME) and superelastic effect (SE) [1]. These characteristics are due to the martensitic transformation and its reversion, which can be activated by thermal or mechanical loads. The two-way shape memory effect (TWSME) is another particular property such that the material is able to remember a geometrical shape at high temperature (above A_f) and another shape at low temperature (below M_f) [1]. During repeated heating and cooling the material changes its shape, in a reversible way, between a hot shape, linked to the austenitic phase, and a cold shape, linked to the martensitic phase. This functional property is observed only after particular training procedures, which produce a dislocation structure [2, 3]. The dislocation structure creates an anisotropic stress field which benefits the formation of preferentially oriented martensite variants, resulting in a macroscopic shape change during thermal transformation cycles.

Due to the interesting functional and mechanical properties, many research activities have been addressed to the experimental characterization of NiTi alloys in the last few years; most of these works have investigated the effects of thermal and mechanical processes, such as thermal treatments, cold work, cutting and welding techniques, on the SME and SE [4–9]. Some research activities have also been focused on the training procedures and experimental measurements of TWSME in NiTi wires and, in particular, the effects of plastic strain on this functional behaviour have been investigated [10–14]. Furthermore, several mathematical models, able to reproduce the NiTi constitutive behaviour, have been proposed in the literature, which simulate the superelastic behaviour as well as the shape memory effects [15–20].

The aim of this work is to investigate the effects of two different training conditions on the TWSME of Ni–51 at.% Ti sheets, and to develop a numerical model which allows

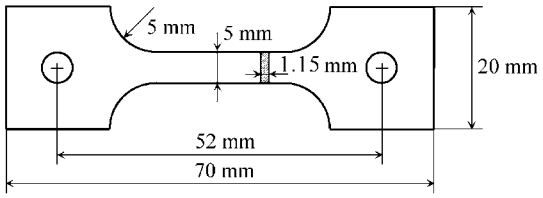

Figure 1. Specimen for the thermo-mechanical cycle.

real time simulations of its hysteretic behaviour strain versus temperature. In particular, the TWSME was induced by a thermo-mechanical cycle which consists in a mechanical loads, up to a training deformation, and a subsequent thermal cycle between the temperatures M_f and A_f. The strain versus temperature hysteresis loops, describing the two-way shape memory behaviour of the material, were measured, and the influence of the training deformation and the number of training cycles were investigated. Furthermore, the TWSME was measured under several values of constant applied stress, and its stability was investigated at increasing number of thermal cycles.

Finally, the measured hysteresis loops were used to develop a numerical model, which is able to describe the hysteretic behaviour of the material. Modelling the hysteretic behaviour of a smart material is not a simple task because the identification of many model parameters is required to adapt the model to the real behaviour of the material. In the last few decades a theory, based on the so-called hysteresis operators, was developed which is able to describe the hysteretic behaviour in a phenomenological way, without considering the underlying physics of the problem. Based on this theory, different models were developed, mainly based on the Preisach [21] and Prandtl–Ishlinskii operators [22–24]. In this work a Prandtl–Ishlinskii operator was used to model the complex hysteretic behaviour of the material and a systematic comparison between experimental measurements and numerical results was carried out.

2. Materials and experiments

Ni–51 at.% Ti sheets 1.15 mm in thickness were used throughout this investigation. The sheets were produced by cold-rolling with a thickness reduction of about 22% and successive thermal treatment at 700 °C for 20 min. Due to the low workability of this class of materials with conventional machining processes, such as milling, turning and drilling, and in order to reduce the extension of the HAZ and the formation of microcracks, the specimens, shown in figure 1, were made by electro-discharge machining [4].

The thermo-mechanical cycles were carried out by using a universal testing machine (Instron 8500), equipped with a furnace (MTS 653). The local deformations of the specimen were measured by a resistance extensometer with a gauge length of 10 mm, while the temperature was acquired, in the middle of the gauge length, by a J-type thermocouple. Load, deformation and temperature outputs were acquired by means of a data acquisition system, represented by a personal computer equipped with a National Instruments acquisition

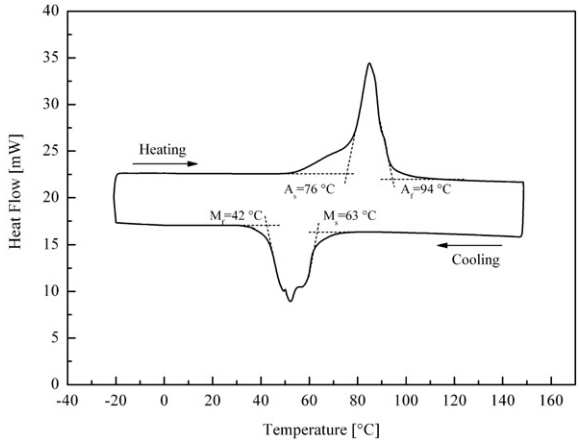

Figure 2. DSC thermogram of the thermally treated material.

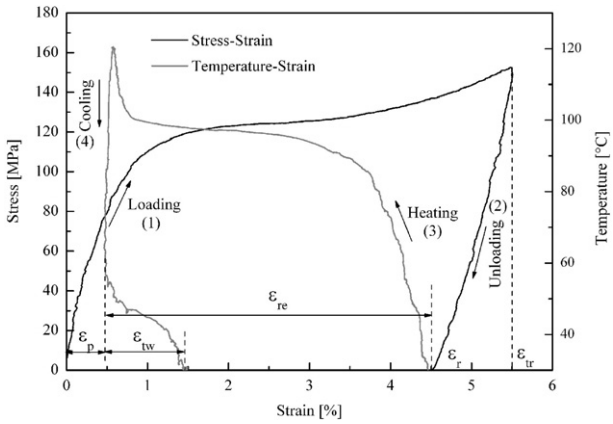

Figure 3. Example of the training cycle.

card (DAQ PCI-MIO16-E-1) controlled by the Labview® 6.0 software package.

In order to identify the temperature range of the thermal cycles, the phase transition temperatures (PTTs) of the thermally treated material were measured by differential scanning calorimetry (DSC) investigations, as shown in the thermogram of figure 2. The tests were carried out under a controlled cooling/heating rate of 5 °C min^{-1}, at temperatures ranging from −20 to 150 °C, and the following values were found: $M_f = 42$ °C, $M_s = 63$ °C, $A_s = 76$ °C and $A_f = 94$ °C.

The training procedure to induce the two-way shape memory behaviour was carried out through the repetition of several thermo-mechanical cycles which produce a dislocation structure. In figure 3 an example of thermo-mechanical cycle is shown, which is composed of four subsequent steps: (1) isothermal (at $T < M_f$) strain controlled uniaxial loading at a strain rate of 0.06 min^{-1} up to a training deformation ε_{tr}; (2) complete isothermal unloading at the same rate and recording the residual strain ε_r; (3) heating up to the austenite finish temperature (A_f) to activate SME and measuring the recovery deformation ε_{re} and plastic strain ε_p; (4) cooling down to the martensite finish temperature (M_f) and recording the two-way shape memory strain ε_{tw}. Several training cycles were carried out for two different values of training deformation, $\varepsilon_{tr} = 3.5\%$

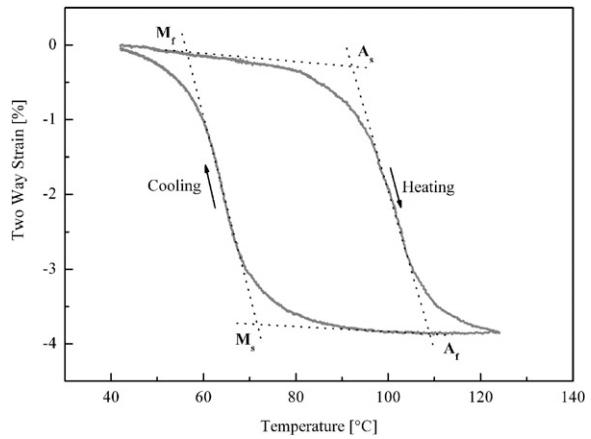

Figure 4. Determination of the phase transition temperatures from the hysteresis loop.

and $\varepsilon_{\mathrm{tr}} = 5.5\%$. Each training cycle starts from the end of the cooling stage of the previous one, so that the total deformation at the ith cycle, $\varepsilon_{\mathrm{tot}(i)}$, can be defined as follows:

$$\varepsilon_{\mathrm{tot}(i)} = \varepsilon_{\mathrm{tr}(i)} + \varepsilon_{\mathrm{p}(i-1)} + \varepsilon_{\mathrm{tw}(i-1)}. \tag{1}$$

The two-way shape memory behaviour of the trained material was measured by a thermal cycle carried out between the transformation temperatures M_{f} and A_{f}. In figure 4 an example of hysteresis loop, two-way strain versus temperature, is shown, which was obtained by measuring the strain during heating the material between M_{f} and A_{f} and subsequently cooling between A_{f} and M_{f}. As shown in the figure the hysteresis loops were used to identify the transformation temperatures of the trained material by the slope line extension method.

3. Numerical model

The experimental measurements, strain versus temperature, describing the two-way shape memory effect, were used to develop a numerical procedure, which is able to model the complex hysteretic behaviour of the material and is efficient enough for use in real-time applications. The model is based on the so-called Prandtl–Ishlinskii operator [22–24]. The basic idea of this approach consists in modelling the hysteretic behaviour by a weighted superposition of many so-called elementary hysteresis operators. These operators have a simple mathematical structure, and are characterized by one or more parameters; one of the most familiar is based on the so-called backlash operator H_r:

$$y(t) = H_r[x, y_0](t) \tag{2}$$

where t represents the time, x and y are the input and output variables, respectively, and y_0 is the initial value of the output. As shown in figure 5(a), the backlash operator is characterized by the control input threshold value r, which is equal to one-half of the deadband width $\mathrm{d}w$.

A generalized backlash operator is obtained by multiplying the backlash operator H_r by a weight value w:

$$y(t) = wH_r[x, y_0](t) \tag{3}$$

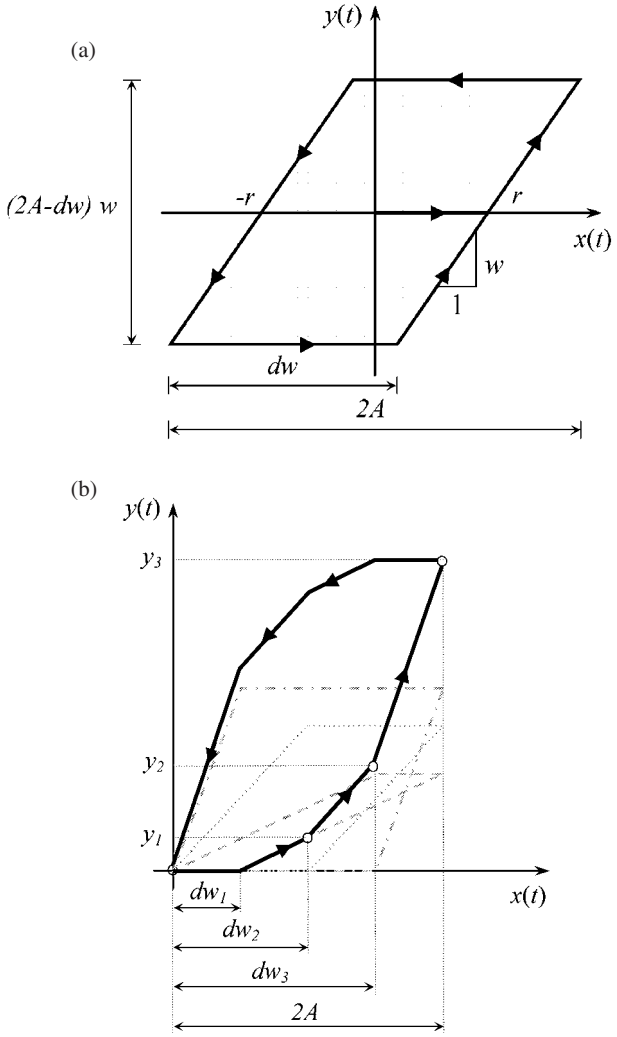

Figure 5. (a) Generalized backlash operator; (b) complex hysteretic loop obtained by a weighted superposition of three backlash operators.

where w defines the gain of the backlash operator and represents the slope of the oblique curve in figure 5(a). The parameter $2A$ in figure 5(a) represents the total amplitude of the input signal.

To obtain a complex hysteretic loop the Prandtl–Ishlinskii hysteresis operator H can be introduced, by a weighted superposition of many elementary operators with different threshold and weight values [22]:

$$H = \{w\}^{\mathrm{T}}\{H_r\} \tag{4}$$

where $\{H_r\}$ is the vector of backlash operators and $\{w\}$ is the corresponding vector of weights. As illustrated in figure 5(b) the proposed approach consists in modelling the hysteretic loop by a linear piecewise discretization; the accuracy of the model can be improved by increasing the total number of linear pieces, which represents the number of the backlash operators. In figure 5(b) three backlash operators are used and they are moved in the origin of the coordinate axis by choosing a proper value of the initial output, $y_0 = \mathrm{d}w/2$, and by subtracting a constant value, equal to $\mathrm{d}w/2$, to the output signal.

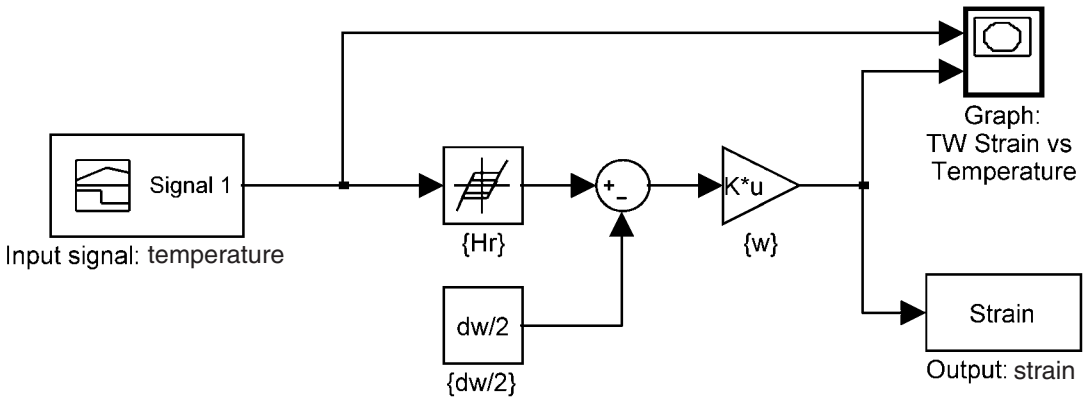

Figure 6. Simulink® model to simulate the TWSME.

The problem of modelling the hysteretic behaviour, starting from the experimental measurements, is now reduced to the determination of the deadband width vector $\{\mathrm{d}w\}$ of the backlash operators and the associated gain vector $\{w\}$. By some geometrical considerations the following simple relation can be used:

$$y_k = \sum_{i=1}^{k} (\mathrm{d}w_{k+1} - \mathrm{d}w_i) w_i \tag{5}$$

where $\mathrm{d}w_i$ represents the deadband width of the generic ith backlash operator; w_i is the corresponding value of the gain; y_k is the output value of the lower branch of the loop in the generic point of discontinuity k (see figure 5(b)). As shown in figure 5(b) the vector $\{\mathrm{d}w\}$ represents a user defined discretization of the total amplitude of the input signal $2A$. Equation (5) can be rewritten in matrix form as follows:

$$\{y\} = [A]\{w\} \tag{6}$$

where the matrix $[A]$ is constructed, for a given $\{\mathrm{d}w\}$ vector, by using equation (5); the unknown vector $\{w\}$ can be found by solving a system of N linear equations, where N is the total number of backlash operators, as follows:

$$\{w\} = [A]^{-1}\{y\}. \tag{7}$$

The above procedure was developed in a Matlab® function, which calculates the model parameters from a set of experimental data describing the hysteretic behaviour of the material. In particular, the function performs the following tasks: (1) partition of the input signal, i.e. the temperature range, and generation of the vector $\{\mathrm{d}w\}$ by a uniform or a non-uniform discretization, in order to distribute a larger number of operators around the nonlinear part of the loop; (2) determination of the matrix $[A]$ of equation (6) by using equation (5); (3) determination of the vector $\{y\}$ by fitting the experimental data; (4) determination of the vector $\{w\}$ by using equation (7). The Simulink® model illustrated in figure 6 was developed and it is efficient enough for use in real time simulation of the TWSME; the model consists of a backlash block $\{H_r\}$, which is defined by the deadband width vector $\{\mathrm{d}w\}$, connected in series with a gain block, which represents the weight vector $\{w\}$ of equation (4), while the constant block $\{\mathrm{d}w/2\}$ allows us to move the backlash operators in the origin of the coordinate axis.

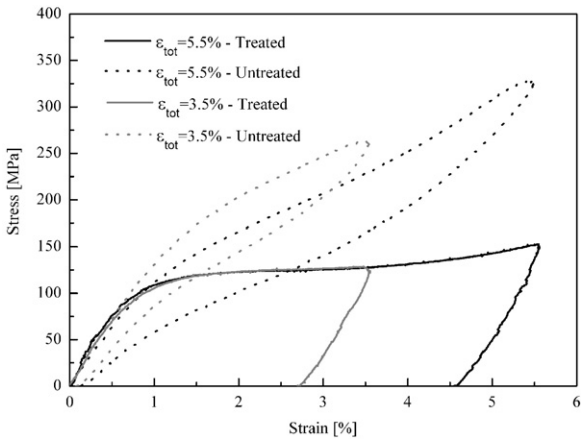

Figure 7. Stress–strain response of the thermally treated material and the untreated one.

4. Results and discussion

4.1. Mechanical characterization and thermal treatment

In this section the mechanical characterization of the material, in terms of the stress–strain curve, is reported. The effects of thermal treatments (700 °C for 20 min) on the stress–strain behaviour are also illustrated by a comparison between treated and untreated material.

In figure 7 the isothermal stress–strain curves, at room temperature, of the treated and untreated materials are shown for two different values of the total deformation ($\varepsilon_{\mathrm{tot}} = 3.5\%$ and 5.5%). The dashed curves show a pseudo-elastic behaviour of the untreated material, but the characteristic stress plateau, due to the $A \rightarrow M$ stress induced phase transformation, is not clearly evident. This behaviour is probably due to the cold-rolling process carried out during the production of the material. The stress–strain response of the thermally treated material is represented by the continuous curves in figure 7; these curves clearly show the shape memory behaviour of the material, as a consequence of the reorientation plateau, due to the detwinning deformation mechanism of the martensite structure, which occurs at a stress level of about 120 MPa.

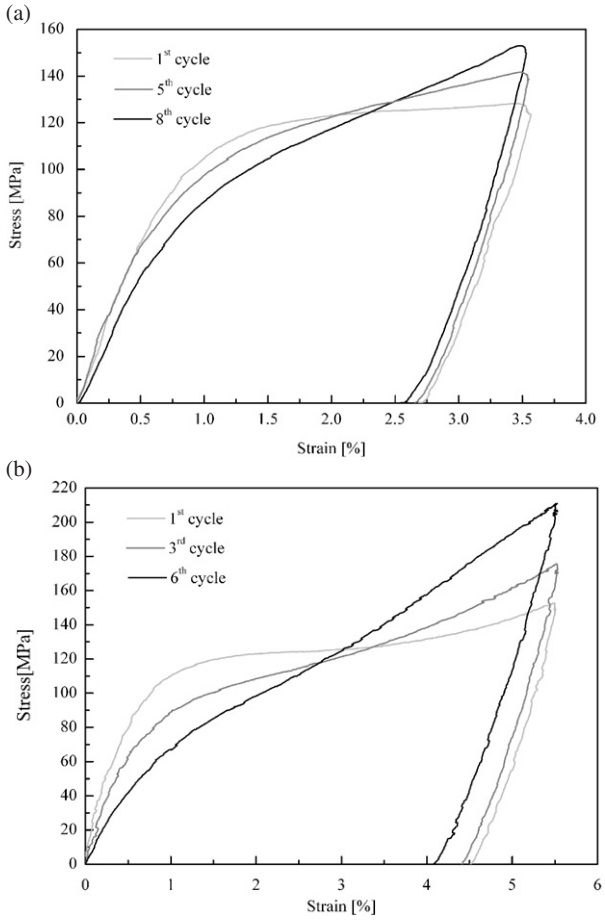

Figure 8. Stress–strain curves during training cycling: (a) deformation training $\varepsilon_{tr} = 3.5\%$; (b) deformation training $\varepsilon_{tr} = 5.5\%$.

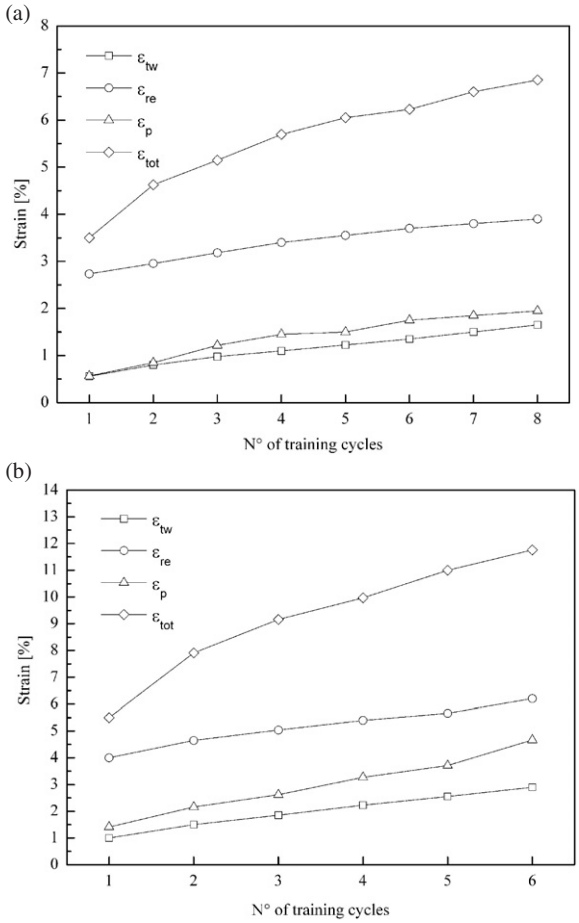

Figure 9. Total strain ε_{tot}, recovery strain ε_{re}, two-way strain ε_{tw} and plastic strain ε_p versus number of training cycles: (a) training deformation $\varepsilon_{tr} = 3.5\%$; (b) training deformation $\varepsilon_{tr} = 5.5\%$.

4.2. Training and two-way shape memory behaviour

The modification of the stress–strain response, during thermo-mechanical training, is shown in figure 8; in particular, figures 8(a) and (b) illustrate the results for $\varepsilon_{tr} = 3.5\%$ and $\varepsilon_{tr} = 5.5\%$, respectively. Eight subsequent training cycles were carried out with $\varepsilon_{tr} = 3.5\%$, while six cycles were executed with $\varepsilon_{tr} = 5.5\%$ in order to avoid fracture, due to the high values of stresses and plastic deformations. Both figures show the stress–strain curves for the first, an intermediate and the last thermo-mechanical cycle; the following observations can be drawn: when increasing the number of training cycles a hardening of the material is observed, resulting in a large stress level, together with a decrease in the stress for the onset of the detwinning. As shown in figure 8(b) this effect is more evident when the material is subjected to a training deformation of 5.5%, resulting in a high slope of the reorientation plateau after six cycles. However, this undesired effect, which is due to the formation of a dislocation structure [2, 3], benefits the two-way shape memory behaviour of the material, as illustrated in the following.

Figure 9 reports the measured ε_{tw}, ε_p, ε_{re} and ε_{tot} versus the number of training cycles, for the two values of training deformation. In particular, figures 9(a) and (b) illustrate the results for $\varepsilon_{tr} = 3.5\%$ and $\varepsilon_{tr} = 5.5\%$, respectively. Both the figures clearly show that the two-way shape memory strain, ε_{tw}, increases with increasing the number of training cycles, i.e. when increasing the total strain ε_{tot}, and a similar behaviour is observed for the plastic deformation ε_p and strain recovery ε_{re}.

In particular, figure 9(a) shows that ε_{tw} increases from 0.5% at the first training cycle, to 1.6% after eight cycles, and the corresponding total deformation, ε_{tot}, rises from 3.5% to 6.8%.

As expected figure 9(b), which is relative to a training deformation of 5.5%, shows higher values of two-way shape memory strain; in particular an ε_{tw} equal to 1.0% and 3.0% is observed after the first and the sixth cycle, respectively, and ε_{tot} increases from 5.5% to 11.8%.

The two-way shape memory strain of the material, obtained by a training deformation of 5.5% after six training cycles, was also measured under a fixed applied stress, as illustrated in figure 10. The figure shows the measured hysteresis loops, two-way strain versus temperature, in the case of the stress free condition, together with those obtained by two fixed values of tensile stress, 50 and 100 MPa. As clearly shown, ε_{tw} increases when increasing the applied stress, from 3.0 to 3.6 and 4.2% under 50 and 100 MPa, respectively. This increase can be attributed to two different mechanisms: (i) the

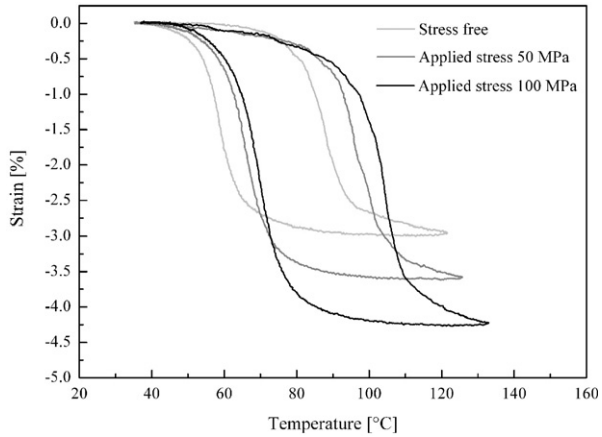

Figure 10. Hysteresis loops at different applied stress.

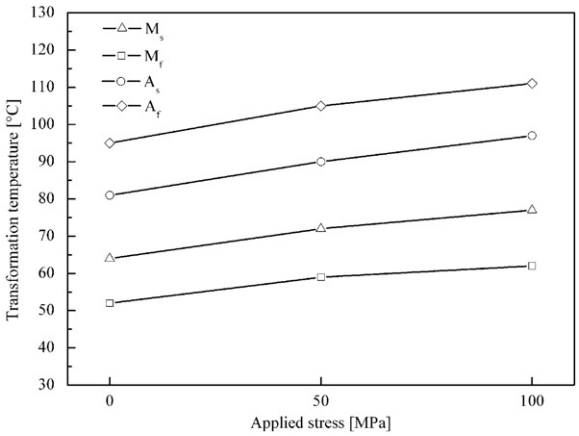

Figure 11. Transformation temperatures as a function of the applied stress.

variation of the Young's modulus in the thermal hysteresis behaviour, between martensite and austenite structure; (ii) the increased volume fraction of favourably oriented martensite variants with increasing external stress [2, 13].

The figure also shows, as expected, a systematic increase of the transformation temperatures [2, 13] because the energy required in the $M \rightarrow A$ transformation increases when increasing the applied stress.

In figure 11 the transformation temperatures as a function of the applied stress are shown.

In particular, an increase of about 10 °C is observed for all transformation temperatures when the specimen is subjected to a tensile stress of 50 MPa, and an increase of about 15 °C is measured in the specimen under 100 MPa.

In many practical applications the NiTi alloys are subjected to many cycles by repeated heating and cooling, therefore the thermal stability of the two-way shape memory effect is an important issue to design and control smart sensors and actuators. In figure 12 the stability of the two-way shape memory effect, for the material obtained by a training deformation of 5.5% after six cycles in the stress free condition, is shown versus the number of thermal cycles.

The material shows a strong reduction of ε_{tw} from about 3.0 to 2.1% after 35 thermal cycles; however, ε_{tw} decreases

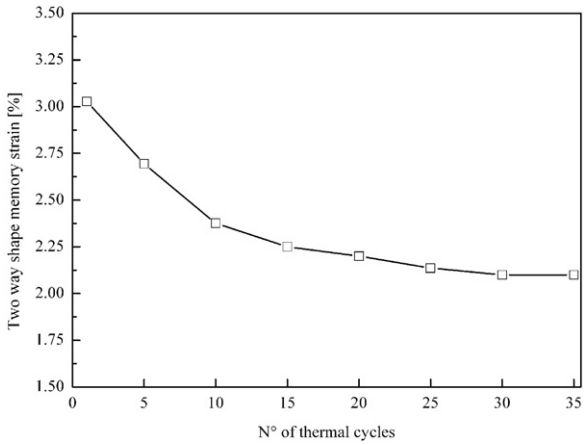

Figure 12. Two-way shape memory strain versus number of thermal cycles.

rapidly in the first 20 thermal cycles and then becomes stable on further increasing the thermal cycles. This behaviour is probably due to a partial relaxation of the stress field formed by the training process, as a consequence of the formation of stabilized martensite [2, 13], leading to a decrease of ε_{tw}.

4.3. Numerical simulation of the hysteresis loops

In this section the accuracy and efficiency of the numerical method described in section 3 is verified through a systematic comparison between numerical simulations and experimental measurements.

Figure 13(a) shows a comparison between an experimentally measured loop in the stress free condition, for the material obtained by a training deformation of 5.5% after six training cycles, and the predictions of the numerical model. The simulation was carried out by using a model with 20 backlash operators equally spaced in the temperature range between 27 and 120 °C, i.e. the vector $\{dw\}$ of equation (5) is obtained by a uniform partition of the temperature range. The figure clearly shows a good accordance between experimental measurements and numerical predictions.

Even if the model with 20 operators shows a sufficiently high efficiency for use in real time applications, the accuracy of the method was investigated by decreasing the total number of backlash operators and by using non-uniform partitions of the temperature range. Figure 13(b) illustrates a comparison between the numerically simulated loops in stress free conditions obtained by models with 20 and 10 operators equally spaced and ten operators non-equally spaced; in particular, larger numbers of operators are used around the nonlinear parts of the loop, i.e. where the curvature is high. As shown in the figure the model with 20 operators uniformly spaced exhibits a very smooth curve, even in the part of the loop with high values of the curvature, while in the model with ten equally spaced operators the linear piecewise discretization is much more evident, resulting in higher numerical errors; finally, the model with ten operators not equally spaced gives a curve very closed to that obtained by the model with 20 operators and a high increase in the accuracy is observed with respect to the prediction of the model with ten equally spaced operators.

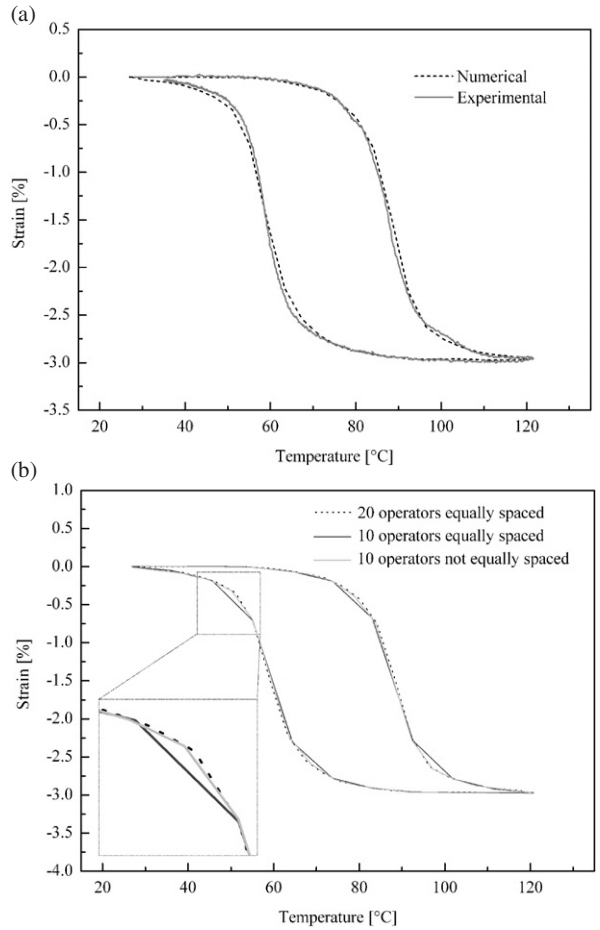

Figure 13. Numerical simulation of the hysteresis loop in the stress free condition: (a) comparison with the experimental loop for a model with 20 operators equally spaced; (b) numerical simulations obtained by models with different numbers of operators.

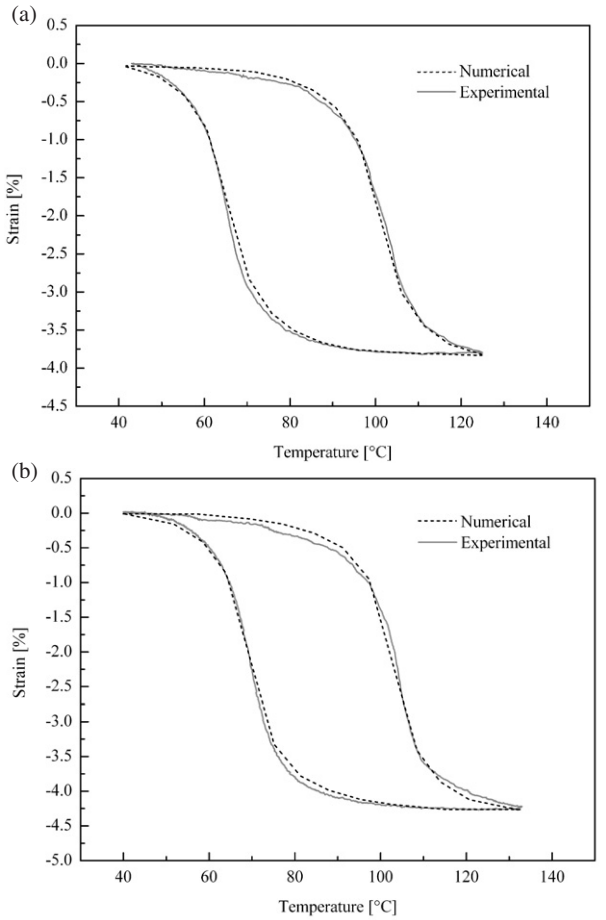

Figure 14. Comparison between experimentally measured loops and numerical simulations for a model with 10 non-equally spaced operators: (a) loop under a constant tensile stress of 50 MPa; (b) loop under a constant tensile stress of 100 MPa.

The accuracy of the model was also verified by simulating the hysteresis loops of the material obtained by a training deformation of 5.5% after six training cycles, measured under two fixed values of tensile stress: 50 and 100 MPa. Figures 14(a) and (b) show the comparisons between the numerically simulated loops and the corresponding experimental measurements under 50 and 100 MPa, respectively; the numerical simulations were carried out by using ten operators not equally spaced. Also in this case the figures clearly show a satisfactory agreement between numerical predictions and experimental data; therefore, the proposed procedure is able to design and control smart sensors and actuators made of NiTi alloys, under different operating conditions, i.e. under different values of applied stress. Further works should be addressed to modify the Prandtl–Ishlinskii hysteresis operator in order to improve the accuracy of the model.

5. Conclusions

In the present work the two-way shape memory effect of a Ti rich NiTi alloy, induced by martensite deformation, was investigated and a numerical model was developed, which allows real time simulations of its hysteretic behaviour of strain versus temperature. In particular a training procedure, which consists in the repetition of several thermo-mechanical cycles, was carried out for two values of training deformation, 3.5% and 5.5%. The influence of training deformation and number of training cycles were investigated. The results show that the two-way shape memory strain, ε_{tw}, increases with increasing number of training cycles, with the maximum values of 1.6 and 3.0% for the training deformation of 3.5 and 5.5%, respectively. Furthermore, ε_{tw} was measured under fixed applied stresses and an increase was observed when increasing the stress, together with an increase in the transformation temperatures. The stability of the two-way shape memory effect was also analysed through the repetition of several thermal cycles and a strong decrease of the ε_{tw} was observed in the first 20 cycles, while it became stable on further increasing the thermal cycles. The proposed numerical model is based on a Prandtl–Ishlinskii operator and was developed in a Matlab® function and a Simulink® model, which simulate the hysteretic behaviour of the material in a phenomenological way by a weighted superposition of several backlash operators. The accuracy and the efficiency of the model were investigated by changing the number of model parameters, i.e. the total number of backlash operators, and by using both uniform and non-uniform partition of the temperature range.

The comparisons between experimentally measured loops, strain versus temperature, and the corresponding numerical predictions show satisfactory agreements, either in simulating the two-way shape memory effect in the stress free condition or under applied stress. The model also shows a sufficiently high efficiency for use in real time applications, therefore it is able to design and control smart sensors and actuators made of NiTi alloys.

References

[1] Schwartz M S 2002 *Encyclopedia of Smart Materials* (Canada: Wiley)
[2] Otsuka K and Ren X 2005 *Prog. Mater. Sci.* **50** 511
[3] Liu Y, Liu Y and Van Humbeeck J 1998 *Acta Mater.* **47** 199
[4] Theisen W and Schuermann A 2004 *Mater. Sci. Eng.* A **378** 200
[5] Schlossmacher P, Haas T and Shussler A 1997 *J. Physique* IV **C5** 251
[6] Tuissi A, Besseghini S, Ranucci T, Squatrito F and Pozzi M 1999 *Mater. Sci. Eng.* A **273–275** 813
[7] Falvo A, Furgiuele F and Maletta C 2005 *Mater. Sci. Eng.* A **412** 235
[8] Falvo A, Furgiuele F and Maletta C 2007 Functional behaviour of a NiTi welded joint: two-way shape memory effect *Mater. Sci. Eng.* A at press
[9] Ming Wu H 2002 *Mater. Sci. Forum* **394/395** 285
[10] Miller A D and Lagoudas D C 2000 *Smart Mater. Struct.* **9** 640
[11] Wada K and Liu Y 2005 *Smart Mater. Struct.* **14** 273
[12] Meng X L, Zheng Y F, Cai W and Zhao L C 2004 *J. Alloys Compounds* **372** 180
[13] Liu Y 1999 *Mater. Sci. Eng.* A **273–275** 668
[14] Luo H and Abel E W 2006 *Smart Mater. Struct.* **15** 1235
[15] Tanaka K 1986 *Res. Mech.* **18** 251
[16] Liang C and Rogers C A 1990 *J. Intell. Mater. Syst. Struct.* **1** 207
[17] Brinson L C 1993 *J. Intell. Mater. Syst. Struct.* **4** 229
[18] Auricchio F and Petrini L 2004 *Int. J. Numer. Methods Eng.* **61** 807
[19] Marfia S, Sacco E and Reddy J N 2003 *AIAA J.* **41** 100
[20] Selden B, Cho K and Asada H H 2006 *Smart Mater. Struct.* **15** 642
[21] Ge P and Jouaneh M 1997 *Precis. Eng.* **20** 99
[22] Krejci P and Kuhnen K 2001 *Control Theory Appl.* **148** 185
[23] Kuhnen K and Janocha H 2001 *Control Intell. Syst.* **29** 74
[24] Kuhnen K 2003 *Eur. J. Control* **9** 407